Journal of Chemical and Petroleum Engineering (JChPE)

Print ISSN: 2423-673X Online ISSN: 2423-6721

Optimization of the Sono-Biodiesel in the Attendance of ZnO Nanoparticles, Process Yield Enhancement: Box Behnken Design

Basir Maleki, S. Siamak Ashraf Talesh *

1. Department of Chemical Engineering, Faculty of Engineering, University of Guilan, Rasht, Iran. E-mail: basir.maleki1368@gmail.com
2. Department of Chemical Engineering, Faculty of Engineering, University of Guilan, Rasht, Iran. E-mail: s_ashraf@guilan.ac.ir

ARTICLE INFO

Article History:
Received: 07 September 2021
Revised: 02 November 2021
Accepted: 03 November 2021

Article type: Research

Keywords:
Biodiesel,
Heterogeneous Catalyst,
Kinetic,
Optimization,
Ultrasonication,
ZnO Nanoparticles

ABSTRACT

The growing fuel demands and drastic restrictions of politics on greenhouse gas emissions are motivating bioenergy research. In this paper, the yield improvement of the produced biodiesel from canola oil using the transesterification process, in attendance of ZnO nanocatalyst and ultrasound waves, was investigated. The crystal size, morphology, and particle size of the prepared nanoparticles were recognized by applying X-ray diffraction (XRD), scanning electron microscopy (SEM), and transverse electron microscopy (TEM) analyses, respectively. The size of ZnO nanoparticles was 45 nm with a hexagonal-shaped structure. The response surface methodology (RSM) and the Box Behnken design (BBD) were employed to analyze the impact of the independent variables on biodiesel production yield. The reliability of the proposed model was verified by applying the analysis of variance (ANOVA) to evaluate response. Regarding the yield, satisfactory accordance was obtained between the calculated and prognosticated data from RSM, with R^2= 0.9910 and R^2 adj= 0.9748. The optimum reaction conditions were acquired at a methanol to oil molar ratio of 11.19:1 mol: mol, ultrasound irradiation time of 31.98 min, and nanocatalyst amount of 3.17 wt.%. The optimum value for the sono-biodiesel yield was achieved equal to 90.16%. Moreover, the kinetic study exhibited that the values of activation energy and Arnius frequency factor were achieved 46.23 kJ mol^{-1} and 5.83× 10^5 min^{-1}, respectively. Accordingly, this research indicated that ZnO nanoparticles can be utilized as a promising and efficient heterogeneous catalyst for biodiesel production.

Introduction

Sustainable fuel sources have currently been developed because of the growing demand and decrease of non-renewable fuels [1]. Among all biofuels, biodiesel has engrossed much regard from both production and research areas, because of its diverse and outstanding benefits [2]. Accordingly, biodiesel is globally growing as engaging bioenergy because it will decrease the greenhouse consequences and aspects of universal warming, as compared to other fuels [3]. The transesterification process causes the production of mono-alkyl esters and glycerol in the presence of a catalyst [4]. Nowadays, advanced and efficient catalyst utilization is emerging to promote the transesterification process of various oils. The type of the applied catalyst in

* Corresponding Author: S. S. Ashraf Talesh (E-mail address: s_ashraf@guilan.ac.ir)

Journal of Chemical and Petroleum Engineering, 2022, 56(1): 1- 14.
Publisher: University of Tehran, College of Engineering DOI: 10.22059/JCHPE.2021.330251.1361

biodiesel production plays an outstanding role in the performance and the reaction rate [5]. Two types of catalysts, i.e., homogeneous and heterogeneous ones, are generally employed for transesterification reactions [6]. Regardless of some benefits of homogenous catalysts in the transesterification process, the reaction has been challenged due to the severe saponification reaction which happens because of the application of this catalyst type [7]. Heterogeneous catalyst is more selected compared to the homogeneous one because of its corrosive essence, the challenge in the separation of homogeneous catalysts, and the enormous wastewater produced after leaching the alkyl ester [8]. Moreover, heterogeneous catalysts, because of the creation of active alkoxide anions on the surface of the catalyst, reveal excellent catalytic activity compared to homogeneous catalysts [9]. The literature review exhibited that many types of research have been carried out to improve biodiesel production in the attendance of heterogeneous catalysts [10]. Furthermore, it has been demonstrated that ZnO nanoparticles exhibit suitable catalytic activity in biodiesel production [11]. Essentially, it is so notable to synthesize a useful heterogeneous base catalyst that could be applied to ameliorate the biodiesel production process [12]. Due to the presence of immiscible phases in the reactor, the contact surface is reduced. Consequently, the rate of transesterification would also experience a remarkable reduction. Therefore, it is essential to intensify the process rate by applying an intense blending association with a heterogeneous catalyst [13]. Hence, reaction through ultrasound-assisted technique can be regarded as an appropriate method to carry out the process. The origins of the sono-chemical method are cavitation generation, growth, and the severe destruction of cavitation droplets in the sono-reactor [14]. Droplets' cavitation because of the production of the collapse waves, free radicals, and jets stream leads to an increase in transesterification development. Hence, ultrasonic wave radiation may expedite the process rate by giving the essential energy to begin the reactions [15]. Besides, ultrasound radiation generates a severe mixing of the reactants in the sono-reactor, which causes mass transfer enhancement [16, 17]. Fig. 1 demonstrates the transesterification reaction through ultrasonic cavitation on the surface of a heterogeneous nanocatalyst.

In the current study, the efficiency of ZnO nanoparticles in attendance of ultrasound irradiation was considered to enhance the yield of canola methyl ester. In this regard, ZnO nanoparticle was prepared using the sol-gel procedure. Crystal size, morphology, and particle size of the prepared ZnO nanoparticles were identified utilizing XRD, SEM, and TEM analysis. Besides, the impact of the empirical conditions, i.e. methanol to oil molar ratio, ultrasonic irradiation time, and nanocatalyst amount were examined on the yield of sono-biodiesel. Statistical analysis was performed to find the relationship between variables of the transesterification process employing the RSM. Therefore, RSM based on the BBD technique was employed to optimize the sono-biodiesel production considering the operating variables. Furthermore, the kinetic survey of canola oil transesterification in the presence of ZnO nanoparticles was investigated in the presence of ultrasound irradiation.

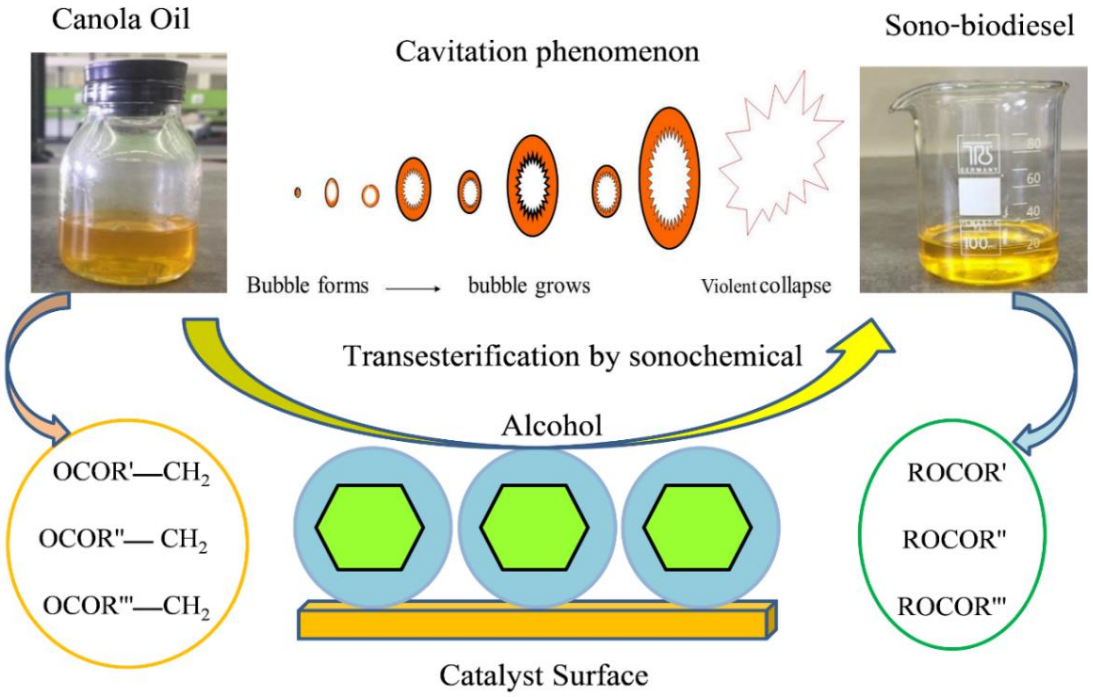

Fig. 1. Transesterification reaction by ultrasonic irradiation on the surface of a heterogeneous nanocatalyst

Materials and Methods

Materials

Zinc acetate (Zn $(CH_3COO)_2.2H_2O$), methanol, and sodium hydroxide (NaOH) were applied to prepare heterogeneous catalysts. Besides, methanol and canola oil were utilized for the biodiesel production reaction. The compositions and Physico-chemical specifications of pure canola oil are displayed in Table 1.

Table 1. Properties of canola oil [18]

Test	Analysis result
Density (g. cm^{-1}@ 15 °C)	0.881
Viscosity ($mm^2.s^{-1}$ @ 40 °C)	29.68
Saponification number (mg KOH g^{-1})	193.8
Acid number (mg KOH g^{-1})	0.1
Fatty acid composition (wt.%)	
Palmitic acid (C16:0)	3.234
Stearic acid (C18:0)	2.190
Oleic acid (C18:1)	63.285
Linoleic acid (C18:2)	22.741
Linolenic acid (C18:3)	6.284

Preparation of ZnO Nanoparticles

The ZnO nanoparticles were prepared via the sol-gel procedure. Zinc oxide sol was readied by adding (Zn $(CH_3COO)_2.2H_2O$) at a concentration of 1 Molar to methanol. The solution was mingled for 100 min at 60 °C. Afterward, 0.5 Molar of sodium hydroxide solution was blended drop-by-drop, which would lead to shifting the white color of the mixture to the milky. During subsequent deposit production, the suspension was mingled at 25 °C temperature for 70 min.

Afterward, the achieved sol was centrifuged for 20 min at 5000 rpm. Eventually, the collected sediment was dried for 120 min at 150 °C.

Nanoparticles Characterization

To characterize the crystallographic aspects of the nanoparticles, XRD patterns were investigated from 2θ =20 to 80° (1.5405 A0 = λ XRD-BRUKER). Moreover, the morphology and particle size of nanoparticles were recognized by scanning electron microscopy (SEM) and transverse electron microscopy (TEM) analyses (SEM-TE-SCAN and TEM-CM 120 Philips), respectively.

Sono-Biodiesel Production

The transesterification reaction was implemented in a sono-reactor (to a frequency of 20 kHz through the Sono plus bandelin- 2200 instrument). The requisite quantity of triglyceride was put into an agitator and preheated to the demanded temperature. After that, the demanded quantity of the ZnO nanoparticles was combined with methanol until appropriate dispersion. The biodiesel production process was implemented based on various runs of the designed tests. Following the completion process, the nanocatalysts were settled through centrifugation at 4000 rpm for 15 min. Subsequently, the remainder of the methanol surplus in the solution was evaporated through warming in the oven. Ultimately, the amount of the mono-alkyl ester in the biofuel phase was recognized by GC-mass examination (Agilent 6890 N coupled with Agilent 5973N mass spectroscopy instrument, narrow cylinder (60 m - 0.25 mm - 0.25 mm). The sono-biodiesel percentage was measured by Eq. 1 [18, 19]:

$$FFA\ Yield\% = \frac{weight\ of\ biodiesel\ produced\ (gr) \times (FAAE\ from\ GC)}{weight\ of\ canola\ oil\ (gr)} \times 100 \qquad (1)$$

Design of Experiments

In this research, the Box Behnken design was employed for experimental design, optimization, and interaction of parameters specified in the transesterification reaction. The influence of three factors was examined at three surfaces: X_1 (methanol to oil molar ratio), X_2 (ultrasonic irradiation time), and X_3 (nanocatalyst amount). The biodiesel yield was considered a response to the experimental design [20]. Table 2 demonstrates the variables and the range of them to design experiments and achieve the highest sono-biodiesel yield in the transesterification process. A multinomial quadratic equation (as displayed in Eq. 2) was applied to show the assessed response (Y) as an accomplice of the operating variable and their interactions.

$$Y = \theta_0 + \sum_{i=1}^{3} \theta_i X_i + \sum_{i-1}^{3} \theta_{ii} X_i^2 + \sum_{i<j} \theta_{ij} X_i X_j \qquad (2)$$

where Y is the prognosticated response, X_i, θ_0, θ_i, θ_{ij}, and θ_{ii} are the dimensionless significance of the factor, the deviation factor, the linear impact of first-order, the interactive influence for j coefficient, and the quadratic influence or linear factor of the model for synergies between i and j, respectively.

Table 2. Empirical limit and surfaces of the three independent variables utilized in BBD

		levels			
No.	**Variables**	**Sign**	**-1**	**0**	**+1**

1	Molar Ratio (mol: mol)	X_1	9	10.5	12
2	Ultrasonic Time (min)	X_3	25	32.5	40
3	Catalyst amount (wt.%)	X_2	2	3	4

Results and Discussion

Nanocatalysts Characterization Procedures

The XRD patterns of the synthesized ZnO nanoparticles are depicted in Fig. 2. The outcomes demonstrate that the ZnO nanocatalysts produced the diffraction peaks according to the XRD of the JCPDS:36-451 X-ray data file. Furthermore, it is worth noticing that no other pollution is observed in the XRD pattern [21]. Accordingly, in the XRD peaks, it is obvious that 2θ amounts are 33.17^0, 36.51^0, 38.64^0, 49.72^0, 58.93^0, 66.79^0, 70.11^0, 74.32^0, and 76.19^0, which conform to the (101), (002), (100), (102), (110), (103), (200), (112), and (201) reflection levels, respectively. The average particle size of the fabricated ZnO solid particles was determined based on the Scherer equation (Eq. 3) [22]:

$$D = \frac{0.89\lambda}{B\ Cos\theta} \tag{3}$$

where D, λ, B, and θ are the mean crystallite size, the wavelength of the XRD, the entire width at half heights in radians, and angle, respectively. The sharpness of summits and their small width display a substantial grade of crystalline particles.

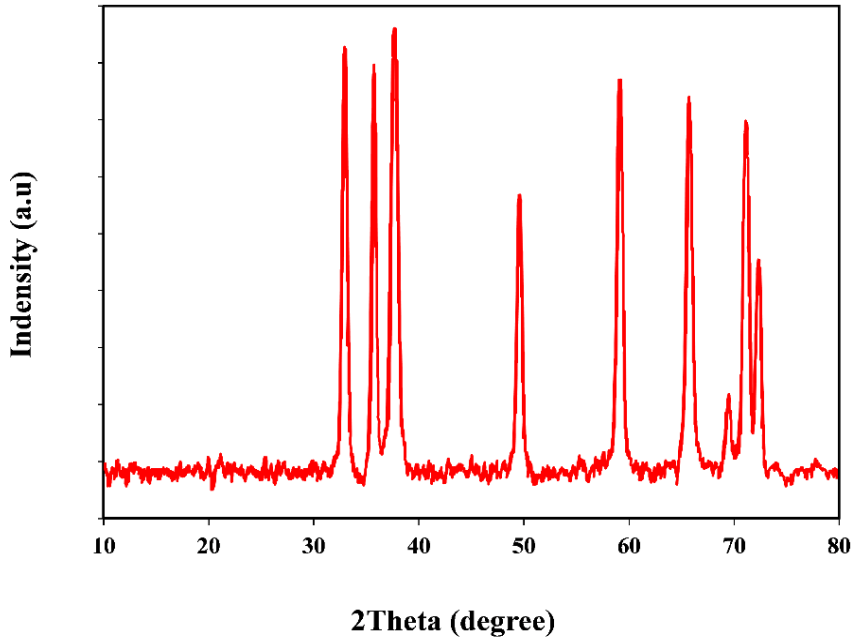

Fig. 2. XRD pattern for ZnO nanoparticles

The morphology, size, and shape of the ZnO nanoparticles are represented in Fig. 3a using transmission electron microscopy analysis. Fig. 3a clearly shows that the size and structure of ZnO solid particles are about 45 nm and have a hexagonal-shaped structure. Moreover, Fig. 3b displays the surface morphology of the prepared nanoparticles. Fig. 3b demonstrates the accumulation of ZnO nanocatalysts with granular cavities. Furthermore, the wall surface of the ZnO nanoparticles was covered with a large quantity of tiny and agglomerated solid particles.

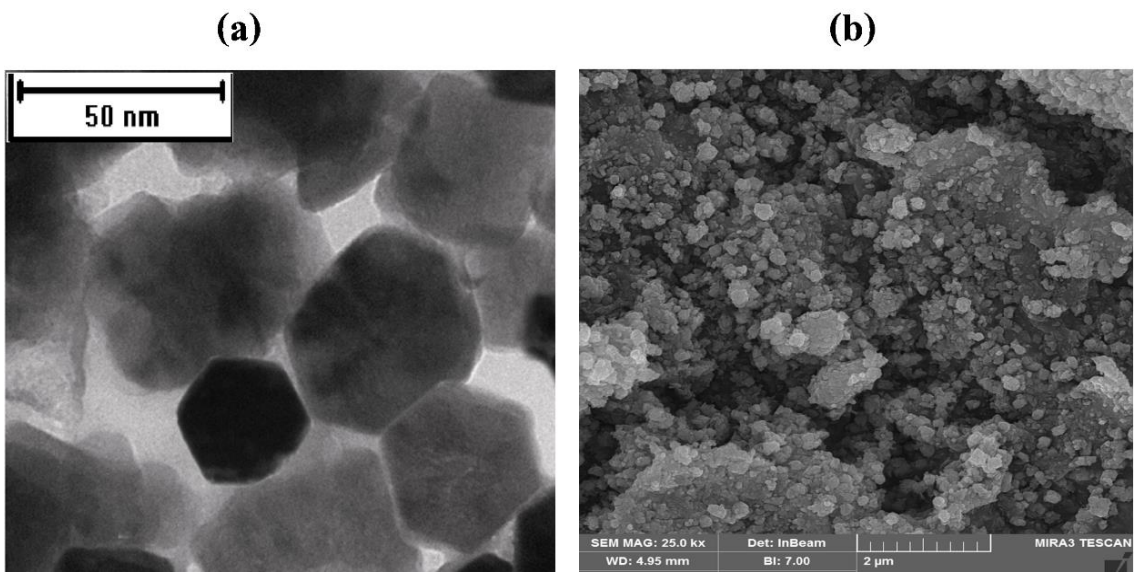

Fig. 3. TEM analysis images (a) and SEM analysis images of nanoparticles (b) of ZnO nanoparticles

Analysis of Sono-Biodiesel Canola Compositions

The results of canola oil to methyl ester quantitative conversion by GC-Mass are exhibited in Table 3. Methyl ester chromatogram of feedstock illustrated the attendance of some certain fatty acid esters, i.e. Palmitic acid (hexadecanoic acid), Stearic acid (octadecanoic acid), Oleic acid ((9Z)-Octadec-9-enoic acid), Linoleic acid ((9Z,12Z)-Octadeca-9,12-dienoic acid), and Linolenic acid ((9Z,12Z,15Z)-Octadeca-9,12,15-trienoic acid). The outcomes of chromatography demonstrated that the canola biodiesel, produced via ultrasonic irradiation-assisted transesterification, proves the attendance of canola methyl esters.

Table 3. Mono-alkyl esters compounds of sono-biodiesel of canola

S. No	Fatty acid	Structure	Chemical Formula	Composition (%)
1	Methyl Palmitate	C16:0	$C_{17}H_{34}O_2$	3.17
2	Methyl Stearate	C18:0	$C_{19}H_{38}O_2$	2.03
3	Methyl Oleate	C18:1	$C_{19}H_{36}O_2$	62.11
4	Methyl Linoleate	C18:2	$C_{19}H_{34}O_2$	21.65
5	Methyl Linolenate	C18:3	$C_{19}H_{32}O_2$	5.84

Validation of the Model using the BBD

According to the selected variables, experimental quantities of the derived sono-biodiesel percentage from canola oil are presented in Table 4. Based on this Table, there was a conspicuous alteration in the biodiesel production percentage under different conditions of the chosen variables. These results reveal that the choice of variables and their limit in the experiment design is well executed.

Table 4. The experimental design and percentage achieved for the sono-biodiesel yield

Parameters				Response
Run	Molar ratio (mol:mol)	Ultrasonic time (min)	Catalyst amount (wt.%)	Yield (%)
1	10.5	25	4	83.12
2	10.5	40	2	81.63

3	10.5	32.5	3	90.06
4	10.5	25	2	87.26
5	9	40	3	74.85
6	10.5	32.5	3	89.52
7	12	40	3	82.34
8	12	32.5	2	88.67
9	12	32.5	4	86.94
10	9	32.5	2	82.27
11	10.5	40	4	84.42
12	9	32.5	4	78.34
13	9	25	3	77.42
14	12	25	3	84.56
15	10.5	32.5	3	89.18

The values of the correlation coefficient (R^2), the adjusted coefficient (R^2_{adj}), and the predicted coefficient ($R^2_{priedicted}$) were accomplished at 0.9910, 0.9748, and 0.9387, respectively. The lack of fit of the suggested model, with a p-value of 0.2063, demonstrated that the lack of fit is not significant and the second-order model is dependable for yield in work. The consequences of the model analysis of variance for the responses are presented in Table 5. In this sense, Prob> F stands for p-value. Besides, values of Prob> F less than 0.05 for each term designate that the term is significant. While values higher than 0.05 show the low importance of terms [23]. According to this criterion, X_1, X_1^2, X_2^2, X_2X_3, and X_2 were meaningful terms of the model related to sono-biodiesel yield. The outcomes of the ANOVA for sono-biodiesel yield, as displayed in Table 5, indicate that X_1 with F-value= 198.85 and <0.0001 p-value has the greatest impact on the response. The precision of the model is assessed by employing a signal-to-noise ratio, in which values more numerous than 4 are acceptable [24, 25]. In the final yield model, the calculated ratio was 24.28, which indicates a very reliable signal for the proposed model. Eventually, the final model (Eq. 4) is manifested in terms of the coded variables for sono-biodiesel yield (Y):

$$Yield\ (\%) = +89.59 + 3.70\,X_1 - 1.14\,X_2 - 0.88\,X_3 + 0.088\,X_1X_2 + 0.55\,X_1X_3 + 1.73\,X_2X_3 - 4.92\,X_1{}^2z - 4.87\,X_2{}^2 - 0.61\,X_3{}^2 \quad (4)$$

Table 5. ANOVA outcomes of the second-order model response surface for the biodiesel yield

Source	sum of squares	Degrees of freedom	average of squares	F-value	p-value
Model	304.01	9	33.78	61.21	< 0.0001
Molar ratio (X_1)	109.74	1	109.74	198.85	< 0.0001
Ultrasonic time (X_2)	10.40	1	10.40	18.84	0.0074
Catalyst amount (X_3)	6.14	1	6.14	11.13	0.0206
$X_1\,X_2$	0.031	1	0.031	0.055	0.8231
$X_1\,X_3$	1.21	1	1.21	2.19	0.1988
$X_2\,X_3$	12.01	1	12.01	21.75	0.0055
X_1^2	89.50	1	89.50	162.17	< 0.0001
X_2^2	87.60	1	87.60	158.73	< 0.0001
X_3^2	1.37	1	1.37	2.48	0.1351
Lack of fit	2.37	3	0.79	4.00	0.2063

Examining the normal probability plot of residuals (Fig. 4b) and the experimental versus predicted value diagrams (Fig. 4b) demonstrates the validity of the acquired model based on a good agreement between the calculated and the prognosticated values. Fig. 4b depicts that the empirical data are uniformly scattered, indicating that the suggested model is reliable. As shown in Figs. 4a and 4b, the points follow the diagonal line and have agreeable distribution.

Furthermore, the residual random scatter distribution between -3 and +3 is observed in Fig 4c, illustrating the satisfactory distribution of data in the design range [26].

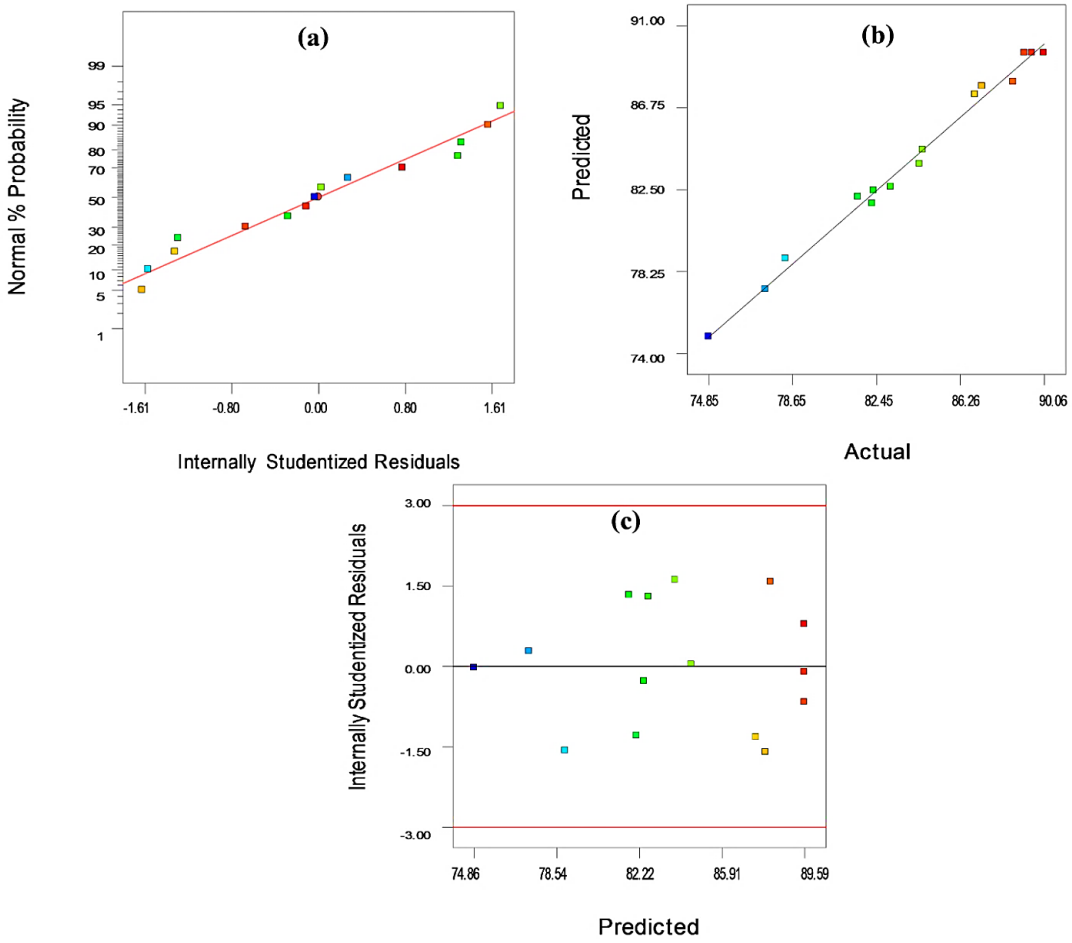

Fig. 4. Plots of the probability of normality (a), predicted experimental values (b), and random dispersion of residuals (c) for sono-biodiesel yield

The Impact of Transesterification Process Parameters

Figs. 5a, 5b, and 5c exhibited the three-dimensional response surface of methanol to oil molar ratio vs. ultrasonic irradiation time, methanol to oil molar ratio vs. nanocatalyst amount, and ultrasonic irradiation time vs. nanocatalyst amount to yield of sono-biodiesel, respectively. The effect of methanol to oil molar ratio and ultrasonic irradiation time on the performance of sono-biodiesel is exhibited in Fig. 5a. In this figure, the nanocatalyst amount was fixed at 3 wt.%. As can be observed from Fig. 5a, with the increase of methanol to oil molar ratio and ultrasonic time, the sono-biodiesel yield was initially increased and then decreased. Furthermore, the highest yield values emerged at X_1 of 11.25 mol: mol, and X_2 were at 32 min. Moreover, as the ultrasonic time rises, the emulsion formation between phases is enhanced and the interface area of the two immiscible phases improves. The acoustic flow and the micro-jet creation would lead to the collapse of bubbles, close to the phase boundary of reactants, and increase the mass transfer coefficient [27].

The interaction effects of the methanol to oil molar ratio, ranging from 9 up to 12 mol: mol, and the nanocatalyst amount, from 2 to 4 wt.% on the sono-biodiesel yield, are illustrated in Fig. 5b. Furthermore, the ultrasonic irradiation time was fixed at 30 min. Based on this figure, the yield gradually ameliorates with the increase of the methanol to molar ratio and nanocatalyst

amount. This is because of the forward reaction development and the production of more methoxide, which breaks down the carbonyl triglyceride bonds and converts them to the sono-biodiesel [28]. The response surfaces in Fig. 5b for catalyst amount revealed that the yield was magnified by increasing the nanocatalyst amount up to 3 wt.% and, then, it began to diminish. This decrease is due to the presence of the excess catalyst and emulsion accumulation of glycerol, which perform it challenging to separate glycerol from sono-biodiesel [29]. Nevertheless, when the catalyst amount increases (up to 3 wt.%), it generates more formation, growth, and destruction of the cavitation bubbles. Hence, these factors intensify the mass transfer coefficient remarkably. It can be observed from Fig. 5c that the ultrasonic irradiation time and nanocatalyst amount have a meaningful impact on the sono-biodiesel yield. According to this figure, the optimal yield occurs when the ultrasonic irradiation time and nanocatalyst amounts are nearly 30 min and 3 wt.%, respectively. If the nanocatalyst amount exceeds 3 wt.%, the accumulation of nanoparticles will lead to the blockage of the activated sites. Therefore, the required surface and orientation for performing the transesterification reaction occurs inappropriately. This phenomenon occurs due to the increase in viscosity of the mixture, which reduces the formation of cavitation droplets and active radicals in the reaction medium [28, 29]. This problem is the main cause of the decrease in sono-biodiesel yield. On the other hand, enhancing the ultrasonic irradiation time through the generation and destruction of cavitation bubbles near the phase boundary enhances the surface contact between the phases and the reaction kinetics [30].

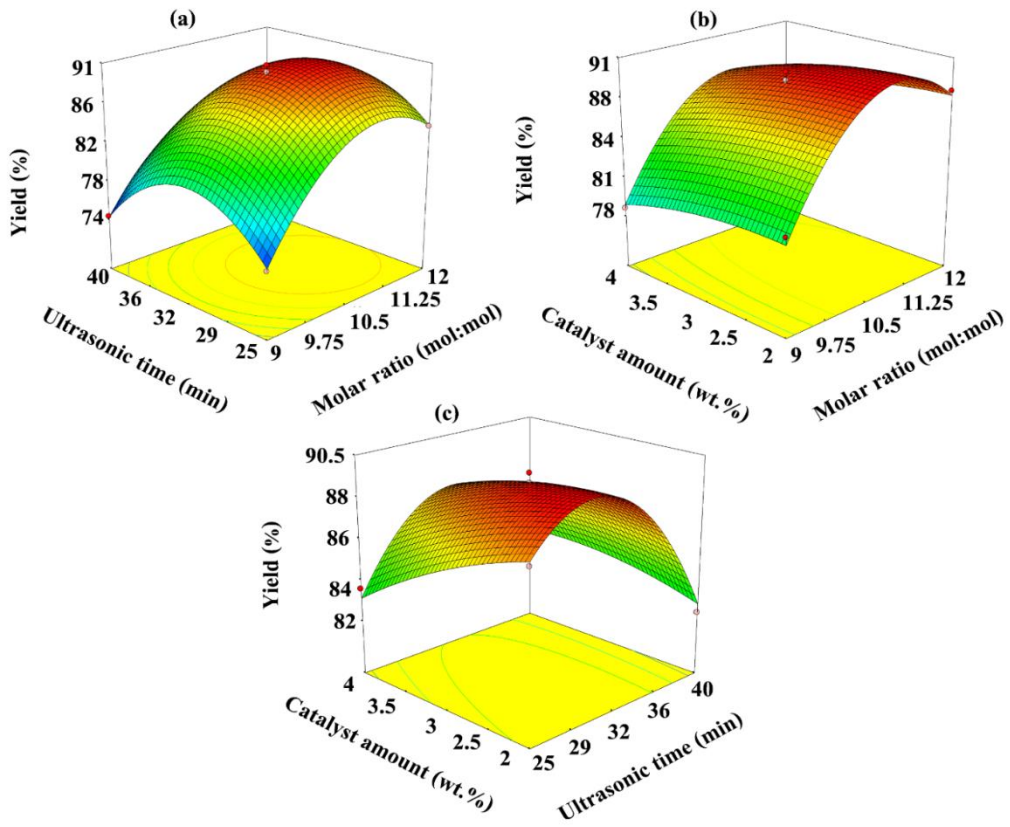

Fig. 5. Response surface and contours associated with the interaction (a) molar ratio and ultrasonic time, (b) molar ratio and catalyst amount, and (c) ultrasonic time and catalyst dosage on sono-biodiesel yield

Optimization

Optimization of the process operating factors was performed by applying statistical evaluation of the BBD approach. Based on Fig. 6, the optimal amount for each parameter is as

regards: methanol to oil molar ratio of 11.19:1 mol: mol, ultrasound irradiation time of 31.98 min, and nanocatalyst amount of 3.17 wt.%. The regression second-order model proved that if the variables obtain these amounts, the maximum sono-biodiesel yield (90.16%) will be accomplished. To validate the measured value, the optimized state was examined thrice and the sono-biodiesel percentage was calculated to be 89.34%. The empirical outcomes illustrated that the value determined by BBD has an excellent accord with experimental data.

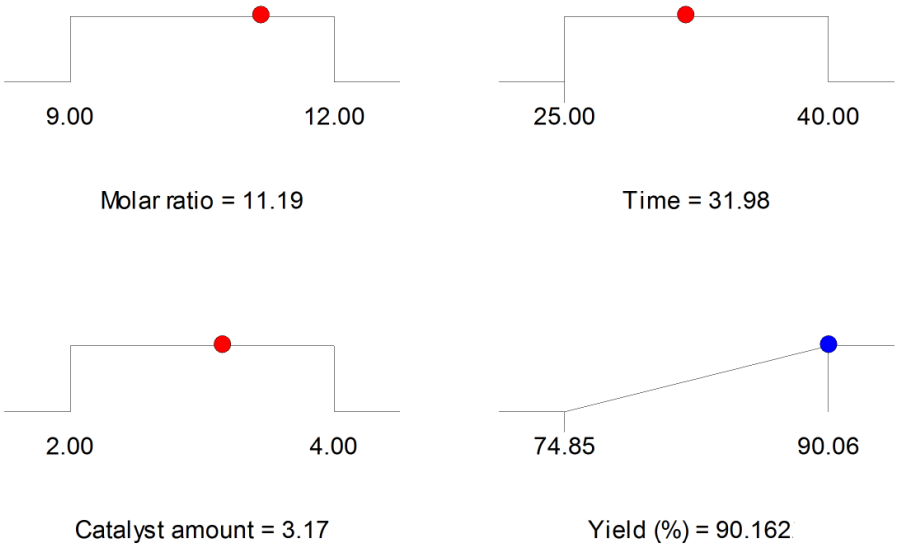

Fig. 6. Optimized values for different values of variables by Box-Behncken method

Kinetic Study

The reaction kinetics investigation was performed under the fixed operating conditions: methanol to oil molar ratio 11.19:1, ultrasonic irradiation times (0 to 30 min), and various nanocatalyst amounts 3.17 wt. %. The kinetic investigation of reaction is according to two assumptions.

1) The rate equation is examined to be a first-order reaction.

2) The reaction rate is subordinate to the canola oil amount that is converted to biofuel. The first-order equation is considered as follows [31]:

$$-ln(1-x) = kt \tag{5}$$

where k, x, and t are the kinetic rate constant (min^{-1}), conversion of oil to biodiesel, and ultrasound irradiation time (min), respectively. The rate constant of a reaction is measured in Fig. 7, confirming that enhancing the rate constant by temperature increment causes biodiesel production amelioration. Ultrasonic irradiation enhances the process kinetics and intensifies the stirring of immiscible phases, remarkably. Therefore, it occurs an increment in the interface during the transesterification, causing a substantial reduction of the mass transfer resistance among the immiscible phases.

$$k = Aexp\left(\frac{-E_a}{RT}\right) \tag{6}$$

where Ea and A are the activation energy ($J.mol^{-1}$) of the reaction and the frequency factor of Arrhenius (min^{-1}), respectively.

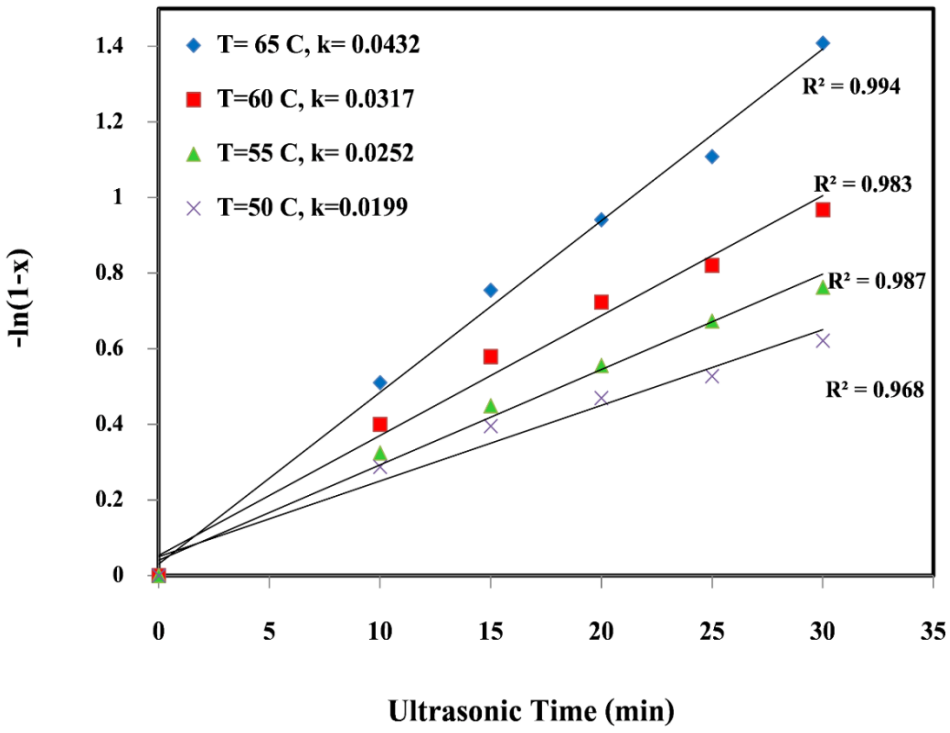

Fig. 7. Reaction kinetics in determining the transesterification reaction rate constant

According to Fig. 8, the activation energy and the frequency factor of the transesterification process were achieved at 46.23 kJ.mol^{-1} and 5.83×105 min^{-1}, respectively. The experimental results confirm that biodiesel production is an endothermic reaction.

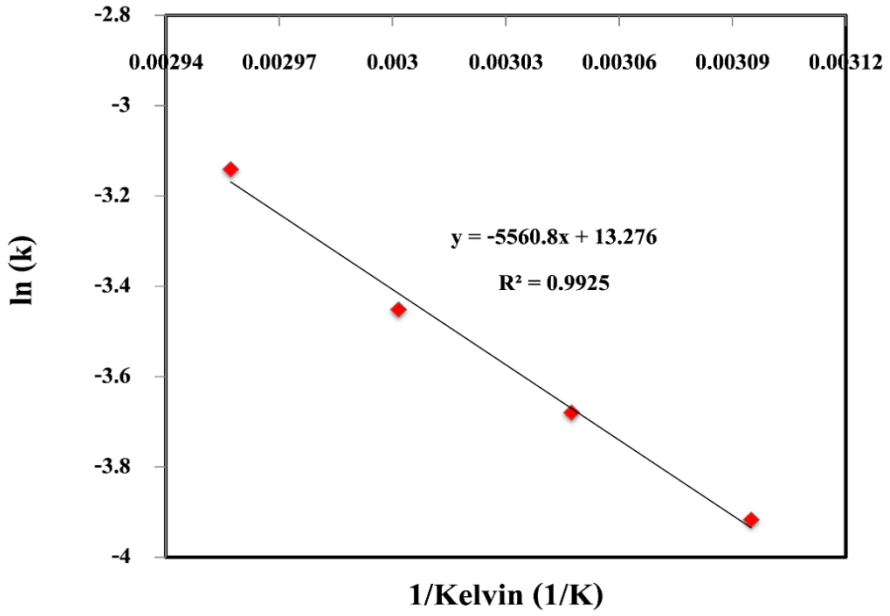

Fig. 8. The evaluation activation energy of process in the attendance of ZnO nanocatalyst

Moreover, the physicochemical features of the optimized sample with a yield of 90.06% are displayed in Table 6. The outcomes reveal that the determined characteristics are within the ASTM standard range [32].

Table 6. Physicochemical properties biodiesel and standards specifications ASTM

Property	ASTM Method	ASTM Specification	Sono-Biodiesel
Specific gravity (gr.cm^{-1}@ 15 °C)	D976	0.860-0.900	0.880
Viscosity (cSt @ 40 °C)	D445	2.5-6	3.89
Acid number (mg KOH g^{-1})	D664	0.5<	0.21
Pour Point (°C)	D97	-15 to +10	-9
Cloud Point (°C)	D2500	-3 to +12	-3
Flash Point (°C)	D93	100>	155
Cetane number	D613	47>	50
Water content (ppm)	D95	500<	262

Conclusion

In the current study, ZnO nanoparticles were prepared via the sol-gel procedure for the biofuel of canola oil in a sono-reactor. Structure and surface attributes were identified via XRD, SEM, and TEM analyses. The main objective of the current study is to achieve the highest yield under optimal reaction conditions. The impact of three quantitative variables, the molar ratio of methanol to oil, ultrasonic time, and catalyst amount on the yield of canola biodiesel produced, were considered. The relationship between reaction variables in biodiesel production was statistically analyzed employing the response level method and Box Bencken design. By performing an analysis of variance, the validity of the acquired quadratic models was confirmed with a precision of R^2 = 0.9910 and R^2_{adj}= 0.9748 for production yield. The results illustrate that the methanol to oil molar ratio strongly affects the produced sono-biodiesel yield. Optimal reaction conditions were achieved in the methanol to triglyceride molar ratio of 11.19:1 mol: mol, ultrasound irradiation time of 31.98 min, and nanocatalyst amount of 3.17 wt.%, respectively. Besides, the kinetic study indicated that the values of activation energy and Arnius frequency factor were achieved 46.23 kJ mol^{-1} and 5.83× 10^5 min^{-1}, respectively. Due to the high capability of ZnO nanoparticles in producing biodiesel to achieve proper efficiency, these nanocatalysts can be employed as heterogeneous catalysts in the production of sono-biodiesel from various oils.

References

[1] Athar M, Zaidi S. A review of the feedstocks, catalysts, and intensification techniques for sustainable biodiesel production. Journal of Environmental Chemical Engineering. 2020;8: 104523.

[2] Foroutan R, Mohammadi R, Razeghi J, Ramavandi B. Biodiesel production from edible oils using algal biochar/CaO/K_2CO_3 as a heterogeneous and recyclable catalyst. Renewable Energy. 2021;168: 1207-1216.

[3] Maleki B, Ashraf Talesh S. S. Optimization of ZnO incorporation to αFe_2O_3 nanoparticles as an efficient catalyst for biodiesel production in a sonoreactor: Application on the CI engine. Renewable Energy. 2022; 182: 43-59.

[4] De A, Boxi SS. Application of Cu impregnated TiO_2 as a heterogeneous nanocatalyst for the production of biodiesel from palm oil. Fuel. 2020; 256: 117019.

[5] S. Banerjee, S. Rout, S. Banerjee, A. Atta, D. Das, Fe_2O_3 nanocatalyst aided transesterification for biodiesel production from lipid-intact wet microalgal biomass: a biorefinery approach, Energy Convers. Management. 2019;195, 844-853.

[6] Rao AVRK, Dudhe P, Chelvam V. Role of oxygen defects in basicity of Se doped ZnO nanocatalyst for enhanced triglyceride transesterification in biodiesel production. Catalysis Communications. 2021; 149:106258.

[7] Suresh T, Sivarajasekar N, Balasubramani K. Enhanced ultrasonic assisted biodiesel production from meat industry waste (pig tallow) using green copper oxide nanocatalyst: Comparison of response surface and neural network modelling, Renewable Energy. 2021;164: 897-907.

[8] Vardast N, Haghighi M, Dehghani S. Sono-dispersion of calcium over Al-MCM-41used as a nanocatalyst for biodiesel production from sunflower oil: influence of ultrasound irradiation and calcium content on catalytic properties and performance. Renewable Energy. 2019; 132: 979–988.

[9] Bai L, Tajikfar A, Tamjidi S, Foroutan R, Esmaeili H. Synthesis of $MnFe_2O_4$@graphene oxide catalyst for biodiesel production from waste edible oil. Renewable Energy. 2021;170: 426-437.

[10] Baskar G, Selvakumari AEI, Aiswarya R. Biodiesel production from castor oil using heterogeneous Ni doped ZnO nanocatalyst. Bioresource Technology. 2018; 250: 793- 798.

[11] Dantas J, Leal E, Mapossa AB, Cornejo DR, Costa ACFM. Magnetic nanocatalysts of $NiO.5ZnO.5Fe_2O_4$ doped with Cu and performance evaluation in transesterification reaction for biodiesel production. Fuel. 2017;191: 463-471.

[12] Santillán-Urquiza E, Arteaga-Cardona F, Hernandez-Herman E, Pacheco-García MPF. Inulin as a novel biocompatible coating: Evaluation of surface affinities toward $CaHPO_4$, a-Fe_2O_3, ZnO, $CaHPO_4$@ZnO and a-Fe_2O_3@ZnO nanoparticles. Journal of Colloid and Interface Science. 2015;460: 339-348.

[13] Jookjantra K, Wongwuttanasatian, T. Optimisation of biodiesel production from refined palm oil with heterogeneous CaO catalyst using pulse ultrasonic waves under a vacuum condition. Energy Conversion and Management. 2017;154: 1-10.

[14] Malani RS, Shinde V, Ayachit S, Goyal A, Moholkar VS. Ultrasound–Assisted Biodiesel Production Using Heterogeneous Base Catalyst and Mixed Non–edible Oils. Ultrasonics Sonochemistry. 2019; 52: 232-243.

[15] Hoseini SS, Najafi G, Ghobadian B, Mamat R, Ebadi MT, Yusaf T. Characterization of biodiesel production (Ultrasonic-assisted) from Evening-primroses (Oenothera lamarckiana) as novel feedstock and its effect on CI engine parameters. Renewable Energy. 2018;130: 50-60.

[16] Selvakumar P, Sivashanmugam P. Ultrasound assisted oleaginous yeast lipid extraction and garbage lipase catalyzed transesterification for enhanced biodiesel production. Energy Conversion and Management. 2019;179: 141-151.

[17] Hoseinia SS, Najafia G, Ghobadiana B, Mamatb R, Ebadia MT, Yusaf T. Ailanthus altissima (tree of heaven) seed oil: Characterisation and optimisation of ultrasonication-assisted biodiesel production. Fuel. 2018; 220: 621- 630.

[18] Maleki B, Ashraf Talesh S.S. Pour point and yield simultaneous improvement of alkyl esters produced by ultrasound-assisted in the presence of αFe_2O_3/ZnO: RSM approach. Fuel. 2021; 298, 120827.

[19] Elango RK, Sathiasivan K, Muthukumaran C, Thangavelu V, Rajesh M, Tamilarasan K. Transesterification of castor oil for biodiesel production: Process optimizationand characterization. Microchem. 2019;145: 1162–8.

[20] Anwar M, Rasul MG, Ashwath N. Production optimization and quality assessment of papaya (Carica papaya) biodiesel with response surface methodology. Energy Conversion and Management. 2018; 156:103-112.

[21] Mohamed MM, Bayoumy WA, El-Faramawy H, El-Dogdog W, Mohamed AA. A novel α-Fe_2O_3/AlOOH (γ-Al_2O_3) nanocatalyst for efficient biodiesel production from waste oil: Kinetic and thermal studies. Renewable Energy. 2020;160: 450-464.

[22] Suryavanshi RD, Mohite SV, Bagade AA, Rajpure KY. Photoelectrocatalytic activity of spray deposited Fe2O3/ZnO photoelectrode for degradation of salicylic acid and methyl orange dye under solar radiation. Materials Science and Engineering: B. 2019 Sep 1;248:114386.

[23] Song X, Li L, Chen X, Xu Q, Song B, Pan Z, Liu Y, Juan F, Xu F, Cao B. Enhanced triethylamine sensing performance of α-Fe2O3 nanoparticle/ZnO nanorod heterostructures. Sensors and Actuators B: Chemical. 2019 Nov 1;298:126917.

[24] Samimi A, Zakeri M, Maleki B, Mohebbi Kalhori D. Experimental and statistical assessments of the mechanical strength reliability of gamma alumina catalyst supports. Particuology. 2015;21: 74-81.

[25] Simsek S, Uslu S. Investigation of the effects of biodiesel/2-ethylhexyl nitrate (EHN) fuel blends on diesel engine performance and emissions by response surface methodology (RSM). Fuel. 2020; 275: 118005.
[26] Singh H, Abhishek Sharma P, Kumar N, Singh Y. Biodiesel yield and properties optimization from Kusum oil by RSM. Fuel. 2021; 291:120218.
[27] Asif S, Ahmad M, Bokhari A, Chuah LF, Klemeš JJ, Akbar MM, Sultana S, Yusup S. Methyl ester synthesis of Pistacia khinjuk seed oil by ultrasonic-assisted cavitation system. Industrial Crops and Products. 2017 Dec 1;108:336-47.
[28] Choudhury HA, Chakma S, Moholkar VS. Mechanistic insight into sonochemical biodiesel synthesis using heterogeneous base catalyst. Ultrasonics sonochemistry. 2014 Jan 1;21(1):169-81.
[29] Kumar G. Ultrasonic-assisted reactive-extraction is a fast and easy method for biodiesel production from Jatropha curcas oilseeds. Ultrasonics sonochemistry. 2017 Jul 1;37:634-9.
[30] Korkut I, Bayramoglu M. Selection of catalyst and reaction conditions for ultrasound assisted biodiesel production from canola oil. Renewable energy. 2018 Feb 1;116:543-51.
[31] Raheem I, Mohiddin MN, Tan YH, Kansedo J, Mubarak NM, Abdullah MO, Ibrahim ML. A review on influence of reactor technologies and kinetic studies for biodiesel application. Journal of Industrial and Engineering Chemistry. 2020 Aug 29.
[32] Ashok A, Ratnaji T, Kennedy LJ, Vijaya JJ, Pragash RG. Magnetically recoverable Mg substituted zinc ferrite nanocatalyst for biodiesel production: Process optimization, kinetic and thermodynamic analysis. Renewable Energy. 2021 Jan 1;163:480-94.

How to cite: Maleki B, Ashraf Talesh SS. Optimization of the Sono-Biodiesel in the Attendance of ZnO Nanoparticles, Process Yield Enhancement: Box Behnken Design. Journal of Chemical and Petroleum Engineering. 2022; 56(1): 1-14.